forests

MDPI

Article

A New Species of *Biscogniauxia* Associated with Pine Needle Blight on *Pinus thunbergii* in China

Changxia Qiao [1], Ruiwen Zhao [1], Dewei Li [2] and Xiaolei Ding [1,*]

[1] Co-Innovation Center for Sustainable Forestry in Southern China, College of Forestry, Nanjing Forestry University, Nanjing 210037, China; qiaocx@njfu.edu.cn (C.Q.); raven97@njfu.edu.cn (R.Z.)
[2] The Connecticut Agricultural Experiment Station Valley Laboratory, Windsor, CT 06095, USA; dewei.li@ct.gov
* Correspondence: dxl@njfu.edu.cn

Abstract: In June 2020, needle blight symptoms on *Pinus thunbergii* were discovered in Bazhong City, Sichuan Province, China. Fungal isolates were obtained from the pine needles of *P. thunbergii*. After examining morphological characteristics and conducting multi-locus (ITS, *ACT*, *TUB2* and *RPB2*) phylogenetic analyses, the isolates SC1–SC5 were determined to be a new species, *Biscogniauxia sinensis*. Genealogical Concordance Phylogenetic Species Recognition with a pairwise homoplasy index test was used to further verify the results of the phylogenetic analyses. The morphology and phylogenetic relationships between this new species and other related *Biscogniauxia* species were discussed. To our knowledge, this is also the first report of *Biscogniauxia sinensis* associated with pine needle blight on *P. thunbergii* in China. The needle damage of *P. thunbergii* associated with *Biscogniauxia sinensis* will detrimentally affect the carbon absorption and photosynthetic efficiency of *P. thunbergii*, further reduce the absorption of nutrients by Japanese black pine and may lead to the imbalance of pine forest conditions, which will have a negative impact on the forest ecological system.

Keywords: Japanese black pine; *Biscogniauxia*; novel taxon; phylogeny; taxonomy; GCPSR

Citation: Qiao, C.; Zhao, R.; Li, D.; Ding, X. A New Species of *Biscogniauxia* Associated with Pine Needle Blight on *Pinus thunbergii* in China. *Forests* **2024**, *15*, 956. https://doi.org/10.3390/f15060956

Academic Editor: Roberto Danti

Received: 27 April 2024
Revised: 23 May 2024
Accepted: 28 May 2024
Published: 30 May 2024

1. Introduction

Pinus thunbergii (Japanese black pine) is native to Japan and Korea and is currently widely distributed in China due to its evergreen attributes, fast growth, and salinity tolerance [1]. It plays essential roles in ecological restoration, such as sand fixation and afforestation [2–4]. Despite the ecological effects, *P. thunbergii* in China were infected by many pathogens, which caused the wilt and mortality of pine trees. For instance, pine wilt disease caused by the pine wood nematode (*Bursaphelenchus xylophilus*) is the most devastating pine disease in China [5]. Needle cast disease caused by *Lophodermium pinastri* was extremely infectious, with a high incidence in young and mature forests. At the early stage, infected needles exhibited yellow spots, then turned to light brown, leading to the abscission of needles. In the spring of the subsequent year, the fallen needles became thin; black horizontal lines emerged and divided the needles into smaller portions. An oval, black fruiting body was then formed between these lines. Upon maturation, these fruiting bodies absorbed moisture, expanded, and developed a central longitudinal fissure, through which ascospores were released [6–8]. Brown-spot needle blight on *P. thunbergii* caused by *Lecanosticta acicola* initially produced small, discolored spots on infected needles, turned brown and died off quickly. The disease started at the base of the crown and gradually spread upward [9]. Such diseases are common with pine needles and also have posed severe threats to the growing conditions of *P. thunbergii*. However, the symptoms of pine needle blight with sporadic black spots are different from these aforementioned diseases.

In June 2020, pine needle blight symptoms were found on *P. thunbergii* at Nanyang Forest Farm, Bazhong city, Sichuan Province, China. Initial observations of discoloration and wilting on black pine needles were made in May, with a significant increase in yellowing

and wilting symptoms occurring in June. The incidence peaked during July and August, coinciding with rising summer temperatures and the onset of the rainy season, sometimes extending into September. This disease progressed rapidly, infecting black pines of various ages and ultimately caused the needles to turn brown, even causing the complete death of the trees. Surveys indicated a disease incidence rate of 30%, signifying a high severity of this disease.

The objectives of this study are to determine a fungus isolated from *Pinus thunbergii* in Sichuan Province with subsequent morphological and phylogenetic analyses. GCPSR with a PHI test was conducted to further justify the placement of this species. Its morphology and molecular differences were compared with known species in the genus.

2. Materials and Methods

2.1. Sampling and Isolation

In total, 20 needles with typical symptoms were collected from Japanese black pines in a pine forest in Bazhong, Sichuan (31°85′88.09″ N, 106°75′36.69″ E (DMS)). All 20 needles were soaked in 1.5% sodium hypochlorite solution for 90 s for surface disinfection and rinsed in sterile water 3 times. The disinfected material was removed using a sterilized scalpel, and disease/health junction parts were cut into 2–3 × 2–3 mm blocks. These tissue blocks were cultivated on 2% potato dextrose agar medium (PDA) and incubated at 25 °C without light [10]. Conidia were removed from colonies with a needle, and pure cultures were obtained by single spore isolation using serial dilution techniques [11]. These pure isolates were stored in the Forest Pathology Laboratory of Nanjing Forestry University. The holotype of the new fungal taxon from this study was deposited at the China Forestry Culture Collection Center (CFCC).

2.2. Colony Observations

Morphological descriptions of the colonies and colony growth rates of isolates were evaluated with PDA and OA. The mycelium block (6 mm in diameter) was placed at the plate center and incubated at 25 °C. Each treatment had five replicates. Colony diameters were measured in perpendicular directions on 5th and 7th days for calculating the growth rate. Color, shape, and texture of the colonies on both sides were recorded.

2.3. Genomic DNA Extraction, PCR, and Sequencing

DNA was extracted from all isolates using the CTAB method [12], and DNA quality and quantity were assessed using Nanodrop, Qubit (Thermo Fisher, Waltham, MA, USA). According to the study on phylogenetic relationship of *Obolarina*/*Biscogniauxia* by Mirabolfathy et al. [13], four loci of ITS, *ACT*, *TUB2* and *RPB2* were amplified and sequenced with primer sets of ITS-5/ITS-4 [14], ACT-512F/ACT-783R [15], Bt2a/Bt2b [16], and fPB2-5F/fPB2-7cR [14], respectively. The polymerase chain reaction (PCR) was performed in a total volume of 20 µL, which contained 1 µL of DNA sample, 1 µL sense primer, 1 µL antisense primer, 7 µL ddH_2O and 10 µL of 2× Green Taq Mix (Table 1). Sequencing of the PCR amplicons was performed by Shanghai Sangon Biotechnology Company.

Table 1. Primers and parameters used for PCR amplification.

Locus	PCR Primers (Forward/Reverse)	PCR: Thermal Cycles: (Annealing Temperature in Bold)
ITS	ITS5/ITS4	95 °C: 5 min, (95 °C: 30 s, **55 °C**: 30 s, 72 °C: 90 s) ×33 cycles, 72 °C: 10 min
ACT	ACT-512F/ACT-783R	95 °C: 2 min, (95 °C: 30 s, **61 °C**: 30 s, 72 °C: 60 s) ×35 cycles, 72 °C: 5 min
TUB2	Bt-2a/Bt-2b	95 °C: 2 min, (95 °C: 30 s, **55 °C**: 30 s, 72 °C: 60 s) ×35 cycles, 72 °C: 5 min
RPB2	fRPB2-5F/fRPB2-7cR	95 °C: 2 min, (95 °C: 30 s, **54 °C**: 30 s, 72 °C: 60 s) ×35 cycles, 72 °C: 5 min

2.4. Morphological Identification

Conidia, conidiogenous cells, and conidiophores were visualized and measured with a Zeiss Axio Imager A2m microscope equipped with Differential Interference Contrast optics (DIC) (Carl Zeiss, Oberkochen, Germany). Microphotographs were taken with ZEN 2 (blue edition, Axio Cam HR R3). The morphological characteristics were described based on the morphology of conidia, conidiogenous cells, and conidiophores [13].

2.5. Phylogenetic Analyses

All nucleotide sequences were searched in NCBI database (https://blast.ncbi.nlm.nih.gov/Blast.cgi (accessed on 15 June 2023) using BLAST toolkit. The BLASTn search based on ITS sequences indicated *Biscogniauxia* sp. SC3 had the highest sequence identity (100%) with *Biscogniauxia maritima* (MN844502). Based on the *TUB2* and *RPB2* sequences, *Biscogniauxia* sp. SC3 showed highest sequence identity with *Biscogniauxia atropunctata* (AY951673, 93.65%) and *Biscogniauxia atropunctata* (JX507778, 96.03%), respectively. While BLASTing with *ACT* sequence, *Biscogniauxia* sp. SC3 had the highest sequence identity (94.98%) with *Obolarina persica* (JX507798). The 72 available ITS sequences of all *Biscogniauxia* taxa were retrieved from the GenBank and a preliminary phylogenetic analysis was conducted using ITS sequences only. Based on the phylogenetic analysis of ITS, 21 closely related taxa with all multi-locus sequences (ITS + ACT + TUB2 + RPB2) were determined and retrieved from GenBank to construct a more reliable phylogenetic tree. The most closely related species outside the study group like *Annulohypoxylon cohaerens* [17] and *Hypoxylon rubiginosum* [18] were chosen as the outgroup [13,19]. The members of the genus *Biscogniauxia* included in phylogenetic analyses were listed in Table 2. BioEdit 7.0.5.3 [20] was used for multiple sequence alignment, clipping and merging to concatenated ITS + *ACT* + *TUB2* + *RPB2* sequence dataset [21]. The concatenated dataset was analyzed in PhyloSuite v1.2.2 [22,23]. ModelFinder was used to choose the most suitable model based on AIC and BIC criteria [24]. Maximum likelihood (ML) analysis was implemented with sequences of multi-loci using IQtree ver. 1.6.8. Bootstrap with 1000 replicates and the GTR + F+I + G4 model were used to improve the assessment of evolutionary branch stability and confidence level in the phylogenetic trees [25,26]. GTR + F + I + G4 model adjusted branch length distribution and the model parameters, until the likelihood value reached maximum. Bayesian Inference (BI) phylogenies were inferred using MrBayes 3.2.6 [27] with SYM + I + G model, 2 parallel runs and 2,000,000 generations. The initial 25% of sampled data were discarded as burn-in. The remaining trees were pooled, and the posterior probabilities (PP) of each branch system as a monophyletic system were calculated. Phylogenetic trees were visualized in FigTree v. 1.4.0 [28].

Table 2. List of *Biscogniauxia* strains used in phylogenetic analysis.

Species	Locality	Host	Strain Number [1]	GenBank Accessions				Reference
				ITS	*ACT*	*TUB2*	*RPB2*	
Annulohypoxylon cohaerens	France	*Fagus*	YMJ 310 = BCRC34013 [ab]	EF026140	AY951766	AY951655	GQ844766	[29]
Biscogniauxia anceps	France	*Fagus*	YMJ 123 = BCRC34029 [ab]	EF026132	AY95178	AY951671	JX507777	[29]
B. anceps	Spain	*Eucalyptus* sp.	CBS 149687 [a]	OQ990096	NA	NA	NA	[30]
B. anceps	England	unknown	KM 201862 [a]	MZ159582	NA	NA	NA	submitted directly
B. arima	Mexico	wood	YMJ 122 * = BCRC34030 [ab]	EF026150	AY951784	AY951672	GQ304736	[29]
B. atropunctata	Ecuador	*Pinus*	NY8660c [a]	HQ108028	NA	NA	NA	submitted directly
B. atropunctata	unknown	Switchgrass	IUB:B.Whitaker:OTU41 [a]	MH178710	NA	NA	NA	submitted directly
B. atropunctata	Canada	*Acer*	KC2031E5 [a]	KX589181	NA	NA	NA	submitted directly
B. atropunctata	unknown	unknown	KoLRI_053373 [a]	MZ855376	NA	NA	NA	submitted directly
B. atropunctata	unknown	milk thistle	G411 [a]	KM215648	NA	NA	NA	submitted directly
B. atropunctata	unknown	unknown	K135 [a]	MK304352	NA	NA	NA	submitted directly
B. atropunctata	unknown	unknown	C226 [a]	MK304016	NA	NA	NA	submitted directly
B. atropunctata	unknown	unknown	W498 [a]	MK247673	NA	NA	NA	submitted directly
B.atropunctata	Iran	*Celtis australis*	BIAT72 [a]	MF497753	NA	NA	NA	submitted directly
B. atropunctata	Mexico	*Taxus globosa*	SGSGf17 [a]	EU715651	NA	NA	NA	[31]
B. atropunctata	USA	wood	YMJ 128 [ab]	JX507799	AY951785	AY951673	JX507778	[13]
B. atropunctata var. *intermedia*	Costa Rica	*Quercus* sp.	B70M = GB 4796 [a]	AJ390412	NA	NA	NA	[31]
B. bartholomaei	USA	branches	ATCC 38992 [a]	AF201719	NA	NA	NA	[32]
B. bartholomaei	USA	branches	108898191 [a]	ON692782	NA	NA	NA	[32]
B. capnodes	China	wood	YMJ 138 = BCRC34032 [b]	EF026131	AY951787	AY951675	JX507779	[29]
B. capnodes	unknown	unknown	S74 [a]	OR237607	NA	NA	NA	submitted directly
B. capnodes	unknown	unknown	FS39 [a]	MF770835	NA	NA	NA	submitted directly
B. capnodes	Gabon	unknown	GAB038 [a]	KY250379	NA	NA	NA	submitted directly
B. capnodes var. *capnodes*	New Zealand	*Lophozonia menziesii*	11682 [a]	MH410019	NA	NA	NA	submitted directly
B. cinereolilacina	Norway	unknown	CBS 10496 [a]	MH862567	NA	NA	NA	[33]
B. citriformis	USA	*Casuarina equisetifolia*	YMJ 129 = BCRC34034 [b]	JX507801	AY951789	AY951678	JX507781	[13]
B. citriformis	China	wood	YMJ 88113012 [ab]	JX507800	AY951790	AY951677	JX507780	[13]
B. cylindrispora	China	*Cinnamomum*	YMJ 89092701 = BCRC33717 [ab]	EF026133	AY951791	AY951679	JX507782	[34]
B. dendrobii	China	*Dendrobium aphyllum*	MFLUCC 17 2607 * [a]	NR172733	NA	NA	NA	[35]
B. formosana	China	Bark	YMJ 89032201 * = BCRC33718 [ab]	JX507802	AY951792	AY951680	JX507783	[34]
B. formosana	unknown	unknown	Gjav1ITS2OTU03662 [a]	KY588559	NA	NA	NA	submitted directly
B. granmo	Austria	*Prunus padus*	YMJ 135 = BCRC34035 [ab]	JX507803	AY951793	AY951681	JX507784	[13]
B. glaucae	China	*Quercus glauca*	GMBC 0007 [ab]	MT624046	MT622656	MT622654	MT622652	[36]
B. latirima	China	Bark	YMJ 89101101 = BCRC33729 [ab]	JX507804	AY951794	AY951682	JX507785	[13]
B. latirima	China	Bark	YMJ 90080703 = BCRC34036 [ab]	EF026135	AY951795	AY951683	JX507786	[29]
B. magna	Thailand	Unidentified	MFLU 18-0850 [a]	MW240616	NA	NA	NA	[37]
B. mangiferae	Thailand	*Mangifera indica*	MFLU 18-0827 *[a]	MN337232	NA	NA	NA	[38]
B. marginata	Switzerland	*Sorbus aucuparia*	ZT-Myc-64233 [a]	MW489534	NA	NA	NA	submitted directly

Table 2. *Cont.*

Species	Locality	Host	Strain Number [1]	GenBank Accessions				Reference
				ITS	*ACT*	*TUB2*	*RPB2*	
B. maritima	Russia	unknown	LE 262845 [a]	JQ247198	NA	NA	NA	submitted directly
B. maritima	Republic of Korea	unknown	KoLRI_EL004708 [a]	MN844502	NA	NA	NA	submitted directly
B. maritima	Republic of Korea	*Parmotrema*	KoRLI046050 [a]	MN341558	NA	NA	NA	submitted directly
B. maritima	Republic of Korea	unknown	KACC 410582 [a]	OR886237	NA	NA	NA	submitted directly
B. marginata	Germany	*Malus* sp.	CBS 124505 [ab]	KU684016	KU684036	KU684124	KU684310	[36]
B. mediterranea	Italy	*Q. pubescens*	B × 70 [a]	KT253502	NA	NA	NA	[39]
B. mediterranea	Italy	*Q. pubescens*	B × 85 [a]	KT253503	NA	NA	NA	[39]
B. mediterranea	France	*Fagus* sp.	YMJ 147 = BCRC34037 [b]	EF026134	AY951796	AY951684	GQ844765	[39]
B. mediterranea	Japan	*Malus* sp.	F8012 [a]	AB693903	NA	NA	NA	submitted directly
B. mediterranea	USA	*Acer*	VH04 [a]	OR778793	NA	NA	NA	submitted directly
B. mediterranea	USA	wood	Kern805 [a]	OP038087	NA	NA	NA	[40]
B. nothofagi	New Zealand	*Lophozonia menziesii*	NZFS 3015 [a]	MN007010	NA	NA	NA	Hood, I.A submitted directly.
B. mediterranea var. *microspora*	Thailand	unknown	BCC 1198 [a]	AB376712	NA	NA	NA	[41]
B. nummularia	England	*Salix alba*	H86 = CCF 3919 [b]	GQ428318	GQ428312	GQ428324	FR715504	[39]
B. nummularia	France	*Fagus* sp.	MUCL 51395 * [a]	JX658444	NA	NA	NA	[39]
B. nummularia	China	unknown	F8422 [a]	ON332160	NA	NA	NA	submitted directly
B. nummularia	Poland	*Viscum album*	122H [a]	OP699770	NA	NA	NA	[42]
B. nummularia	Poland	*Pinus*	Bn5L-19Pu [a]	MN588203	NA	NA	NA	submitted directly
B. nummularia	Iran	*Zelkova*	BINU72 [a]	MF358880	NA	NA	NA	submitted directly
B. cf. *nummularia*	unknown	*Lewinskya*	2010_26_NT2 [a]	MW907969	NA	NA	NA	submitted directly
B. nummularia var. *merrillii*	Thailand	bark	BCC 1213 [a]	AB376714	NA	NA	NA	[41]
B. petrensis	Thailand	*Dendrobium harveyanum*	MFLUCC 14-0151 * [a]	MK951680	NA	NA	NA	[38]
B. cf. *petrensis*	Ecuador	wood	RLC_1445.1_iNat_7002890 [a]	OQ878456	NA	NA	NA	[43]
B. petrensis	Japan	Tea	ST253 [a]	LC685807	NA	NA	NA	submitted directly
B. petrensis	China	*Osmanthus* sp.	HKAS 102388 [a]	MW240615	NA	NA	NA	[37]
B. petrensis	unknown	unknown	X2P3HRa [a]	ON921656	NA	NA	NA	submitted directly
B. philippinensis var. *microspora*	China	Bark	YMJ 89041101 * = BCRC33720 [ab]	EF026136	AY951797	AY951685	JX507787	[39]
B. repanda	USA	*Fagus* sp.	ATCC 62606 [a]	KY610383	NA	NA	NA	[44]
B. repanda	unknown	unknown	B75A [a]	AJ390418	NA	NA	NA	[45]
B. rosacearum	Italy	*P. domestica*	Bx26 = CBS141046 * [a]	KT253493	NA	NA	NA	[39]
B. rosacearum	Italy	*P. domestica*	Bx4	KT253491	NA	NA	NA	[39]
B. rosacearum	Khorramabad	*Quercus. brantii*	IRAN 4288C [a]	MZ359664	NA	NA	NA	[45]
B. rosacearum	Iran	*almond tree*	IRNBS68 [a]	MW452324	NA	NA	NA	[45]
B. rosacearum	unknown	unknown	CSN1052 [a]	MT813910	NA	NA	NA	[46]
Biscogniauxia sinensis	China	*Pinus thunbergii*	SC1 = CFCC59648 [ab]	OR803753	OR832182	OR832177	OR832187	This study
Biscogniauxia sinensis	China	*P. thunbergii*	SC2 = CFCC59649 [ab]	OR803754	OR832183	OR832178	OR832188	This study

Table 2. *Cont*.

Species	Locality	Host	Strain Number [1]	GenBank Accessions				Reference
				ITS	*ACT*	*TUB2*	*RPB2*	
Biscogniauxia sinensis	China	*P. thunbergii*	SC3 = CFCC59650 * $_{ab}$	OR803755	OR832184	OR832179	OR832189	This study
Biscogniauxia sinensis	China	*P. thunbergii*	SC4 = CFCC59651 $_{ab}$	OR803756	OR832185	OR832180	OR832190	This study
Biscogniauxia sinensis	China	*P. thunbergii*	SC5 = CFCC59652 $_{ab}$	OR803757	OR832186	OR832181	OR832191	This study
B. simplicior	France	*Rhamnus cathartica*	YMJ 136 = BCRC34038 $_{ab}$	EF026130	AY951798	AY951686	JX507788	[39]
B. simplicior	unknown	unknown	B73C $_{a}$	AJ3904916	NA	NA	NA	[31]
B. uniapiculata	China	Bark	YMJ 90080608 = BCRC34039 $_{ab}$	JX507805	AY951799	AY951687	JX507789	[39]
B. aff. uniapiculata	Gabon	unknown	GAB220 $_{a}$	KY250378	NA	NA	NA	submitted directly
B. whalleyi	Thailand	wood	SWUF 13-85 $_{ab}$	MW403821	MZ466385	MZ466386	MZ466387	Jantaharn, P. submitted directly.
Hypoxylon rubiginosum	UK	*Fraxinus*	YMJ 24 = BCRC34116 $_{b}$	EF026143	AY951862	AY951751	JX507791	[39]

Note: NA, not applicable. Strains in this study are marked in bold. * = ex-type. $_{a}$ = ITS phylogenetic analyses. $_{b}$ = complete sequences of ITS + *ACT* + *TUB2* + *RPB2*. [1] *MFLUCC*: Mae Fah Luang University Culture Collection, Chiang Rai, Thailand; *MFLU*: Mae Fah Luang University Herbarium, Thailand; *CBS*: Culture Collection of the Westerdijk Fungal Biodiversity Institute, Utrecht, The Netherlands; *CFCC*: China Forestry Culture Collection Center, China; *ATCC*: American Type Culture Collection; *MUCL*: Agro–Food and Environmental Fungal Collection, Belgium; *BCRC*: Bioresource Collection and Research Center, China; *MFLUCC*: Mae Fah Luang University Culture Collection, Chiang Rai, Thailand; *CCF*: Culture Collection of Fungi, Department of Botany, Faculty of Sciences, Charles University, Prague, Czech Republic; YMJ: Yu-Ming Ju's private collection.

2.6. Genealogical Concordance Phylogenetic Species Recognition Analysis

The Genealogical Concordance Phylogenetic Species Recognition (GCPSR) model and paired homology index (PHI or Φw) tests were used to make comparisons between new species and closely related taxa [47]. The PHI tests were applied in SplitsTree4 [48] to identify the level of recombination among closely related species using a four-locus dataset. A PHI index lower than 0.05 threshold (Φw < 0.05) indicated remarkable recombination in the dataset. The association between this new taxon and closely related species was visualized with splits graphs using the LogDet transformation and splits decomposition options [26].

3. Results

3.1. Sampling and Isolation

In June 2020, pine needle blight symptoms were found on *P. thunbergii* at Nanyang Forest Farm, Bazhong city, Sichuan Province, China. The incidence of the disease was ca. 30%, but severe. All infected pine needles showed brownish-yellow necrotic lesions at the tips, then the symptoms gradually spread to the entire pine needles. The pine needles became light brown, chlorotic, dry, and necrotic. In the late stage, infected pine needles defoliated.

Five fungal isolates (SC1, SC2, SC3, SC4 and SC5) with similar colony morphology were obtained from the infected pine needle tissues. The above isolates were used for subsequent phylogenetic analyses, and isolate SC3 was employed for morphology study.

3.2. Phylogenetic Analyses

The phylogenetic analysis using ITS sequences only showed that five fungal isolates (SC1, SC2, SC3, SC4 and SC5) were clustered in an independent clade, and they were closely related with *B. atropunctata* (G411 and SGSGf17), *B. mediterranea* var. *microspora* and *B. nummularia* var. *merrillii* (Figure 1).

The phylogenetic analyses using a four-locus (ITS, *ACT*, *TUB2*, *RPB2*) dataset of *Biscogniauxia* were conducted to verify the above classification result. This data set consisted of 84 sequences, including 21 ITS sequences, 21 *ACT* sequences, 21 *TUB2* sequences and 21 *RPB2* sequences from 17 taxa. Meanwhile, 20 novel sequences from 5 isolates (SC1-SC5) of *Biscogniauxia* sp. were generated from our collections and analyzed. Consequently, phylogenetic analyses were performed with a total of 1911 characters, including gaps that were *ACT*: 1–320, ITS: 321–654, *RPB2*: 655–1507, *TUB2*: 1508–1911. In this phylogenetic tree, five isolates (SC1-SC5) were clustered in a distinct clade with well-supported values (BI/ML = 1/94) (Figure 2), and these isolates differed from all other known species (Figure 2). Notably, this clade had a close relationship with *B. atropunctata* YMJ128. Based on the two aforementioned phylogenetic analyses, the five fungal isolates represented a new species, *Biscogniauxia sinensis* sp. nov.

Figure 1. Phylogenetic relationship of SC1, SC2, SC3, SC4 and SC5 with related taxa in *Biscogniauxia* derived from ITS. The tree is rooted with *Annulohypoxylon cohaerens* (YMJ 310). The values on the branches are Bayesian posterior probability (BI-PP) $\geq$ 0.90 and the ML bootstrap value (BS) $\geq$ 70, respectively. Isolates in this study are highlighted in red and holotype isolates are in bold.

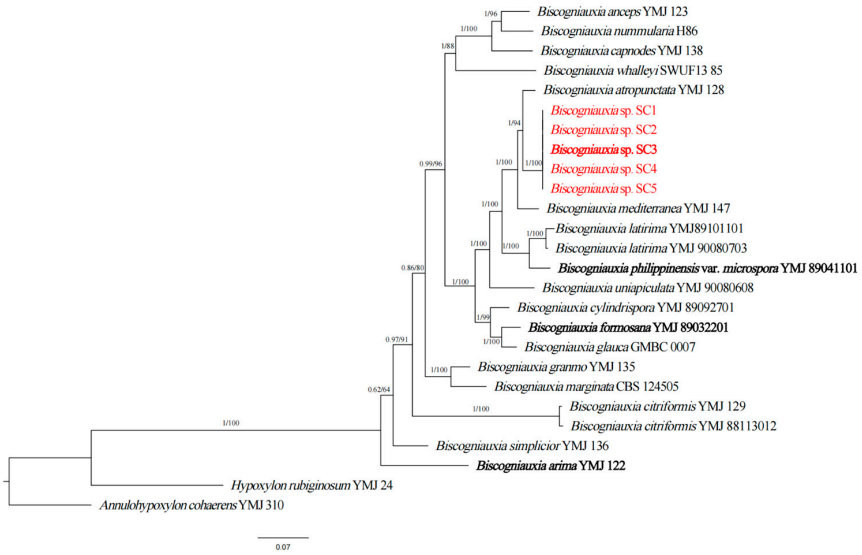

Figure 2. Phylogenetic relationship of five isolates (SC1, SC2, SC3, SC4 and SC5) with related taxa in Biscogniauxia derived from completed squences of ITS, *ACT*, *TUB* and *RPB2*. The tree is rooted with *Annulohypoxylon cohaerens* (YMJ 310) and *Hypoxylon rubiginosum* (YMJ 24). The values on the branches are Bayesian posterior probability (BI-PP) $\geq$ 0.90 and the ML bootstrap value (BS) $\geq$ 70, respectively. Isolates in this study are highlighted in red and holotype isolates are in bold.

3.3. Genealogical Concordance Phylogenetic Species Recognition

The GCPSR principle was applied to evaluate the boundary of different species. The PHI test (Figure 3) on *Biscogniauxia sinensis* showed that there was no significant recombination (Φw = 1.0) between *Biscogniauxia sinensis* and its closely related species, *B. atropunctata* (SGSGf17, B5A, YMJ128).

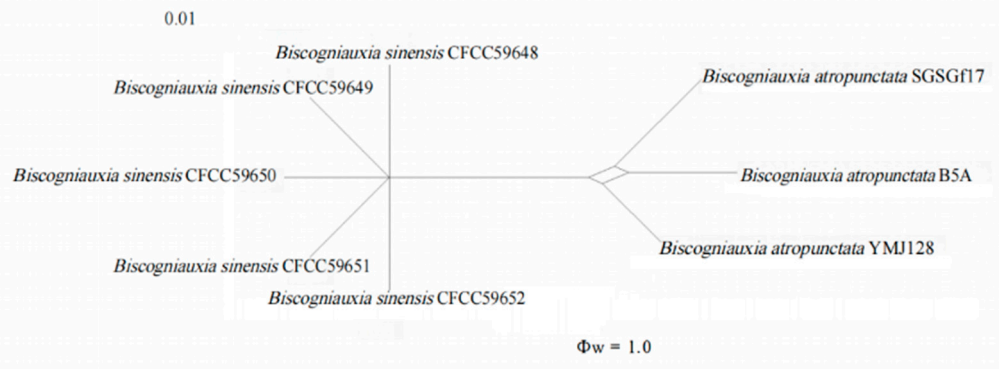

Figure 3. Pairwise homoplasy index test among *Biscogniauxia sinensis* and their closely related taxa.

3.4. Taxonomy

Biscogniauxia sinensis Xiao-Lei Ding, Chang-Xia Qiao and D.W. Li, sp. nov. Figure 3.
Index Fungorum Number: IF 900185.

Etymology: The epithet refers to China where the holotype was collected.

Diagnosis: Differs from *B. atropunctata* in its shorter conidiogenous cells, is light brown and has smaller conidia. Differs from *B. mediterranea* in its smaller conidiogenous cells and shorter conidia. Differs from *B. rosacearum* in its shorter and wider conidia.

Description: The sexual state was not observed in vitro. Conidiophores, which are hyaline to yellowish, often occur on the aerial hyphae, composing of a principal axis and one or more branches, (7.5-) 8.2–11.8 (-13.7) × (1.9-) 2.2–3.0 (-3.6) μm, (mean ± SD = 10.0 ± 1.8 × 2.6 ± 0.4 μm, n = 40), with conidiogenous cells developing terminally, generally two to three. Conidiogenous cells are hyaline, oval, (3.8-) 4.5–6.5 (-7.9) × (2.9-) 3.3–4.1 (-4.5) μm, (mean ± SD = 5.5 ± 1.0 × 3.7 ± 0.4 μm, n = 40), and the apical area has remnants of conidial secession, with the apical end distorted due to producing a large number of conidia. The conidia are hyaline to light brown, globose or subglobose, smooth, and aggregated, (3.3-) 3.5–4.3 (-5.0) × (2.9-) 3.3–3.9 (-4.4) μm, (mean ± SD = 3.9 ± 0.4 × 3.6 ± 0.3 μm, n = 40).

Culture characteristics: Colonies on PDA grow fast, reaching the whole Petri dish in 5 d at 25 °C; they are initially white, cottony, and radial with abundant aerial mycelia and diffuse margins, and become floccose with the reverse side being reddish-brown with brown pigmentation after about 14 d (Figure 4G), even showing no sporulation. Colonies of *Biscogniauxia sinensis* that cover the entire OA Petri dish in 9 d at 25 °C, are regular and round. The mycelia changed from translucent at first to white and turned pale gray with aging. After 15 d, the reverse side became translucent to yellowish (Figure 4H). The mycelium was tight, and the aerial hyphae were raised, white and flocculent. Sporulation formed more frequently on aerial hyphae.

Holotype: China, Sichuan Province, Bazhong city, Nanyang Forest Farm, 31°85′88.09″ N, 106°75′36.69″ E (DMS), isolated from pine needles of *Pinus thunbergii*, June 2020, Xiao-Lei Ding, holotype CFCC59650. The holotype is a living specimen being maintained via lyophilization at the China Forestry Culture Collection Center (CFCC), Chinese Academy of Forestry, Beijing, China, and the ex-type SC3 is preserved at the Forest Pathology Laboratory, Nanjing Forestry University.

Habitat and host: On the pine needles of *Pinus thunbergii* with blight.

Known distribution: Bazhong, Sichuan Province, China.

Additional specimens examined: China, Sichuan Province, Bazhong city, Nanyang Forest Farm, 31°85′88.09″ N, 106°75′36.69″ E (DMS), isolated from a pine needle of

Pinus thunbergii, June 2020, Xiao-Lei Ding, CFCC 59,648 (=SC1), CFCC 59,649 (=SC2), CFCC 59,651 (=SC4), CFCC 59,652 (=SC5).

Note: In the multi-locus phylogenetic tree of the *Biscogniauxia* species, five strains of *Biscogniauxia sinensis* formed a single clade. *Biscogniauxia sinensis* can be distinguished from the closely related species *B. atropunctata*, based on the base-pair differences in ITS (36 out of 469), *ACT* (17 out of 278), *TUB2* (45 out of 520), *RPB2* (47 out of 1133). Morphologically, *Biscogniauxia sinensis* has shorter conidiogenous cells than those of *B. atropunctata* (4.5–6.5 × 3.3–4.1 vs. 5–10 × 3.5–4.5) μm [35]. Conidia are colorless to light brown, which are distinguished from the colorless conidia of *B. atropunctata* [49]. Moreover, *Biscogniauxia sinensis* has smaller conidia (3.5–4.3 × 3.3–3.9 μm vs. 4–5.5 × 3–4.5 μm) than those of *B. atropunctata* [49].

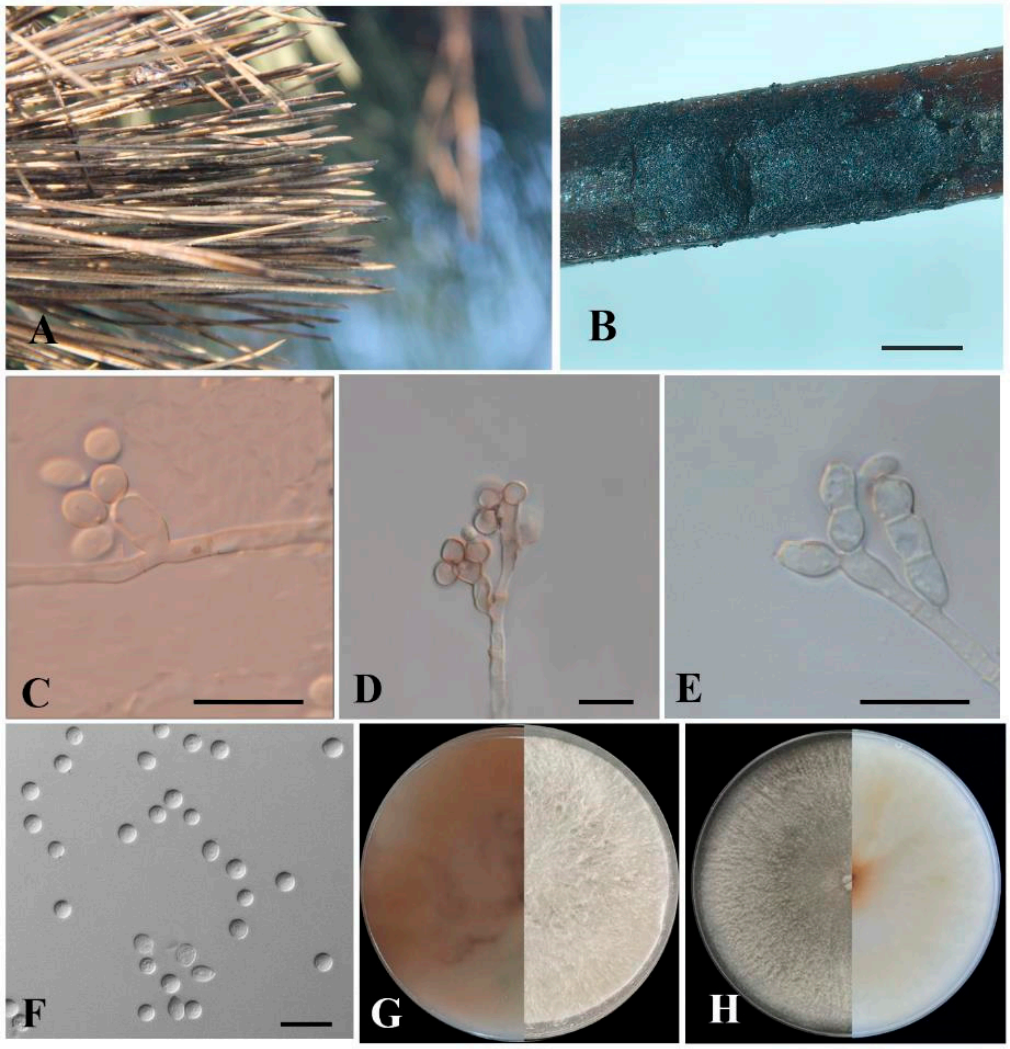

Figure 4. Morphological characteristics of *Biscogniauxia sinensis* from *Pinus thunbergii*. (**A**) Diseased needles in the field. (**B**) Conidiomata on needles. (**C**–**E**) Conidiophores, conidiogenous cells and conidia. (**F**) Conidia. (**G**) Cultures on PDA from above (right) and reverse (left). (**H**) Cultures on OA from above (left) and reverse (right). Scale bars: (**B**) = 500 μm; (**C**–**G**) = 10 μm.

4. Discussion

Based on the morphological features, multi-locus phylogeny, and GCPSR analyses, the five isolates obtained from wilting needles of *P. thumbergii* were identified as a new species. According to the available information, this is also the first report of pine needle blight on *P. thunbergii* associated with *Biscogniauxia sinensis* in China.

It is worth noting that the new species associated with pine needle blight on *P. thunbergii* was closely related with *B. atropunctata* in the multi-locus and ITS-only phylogenetic analyses. By comparing the sequences, there are obvious differences between *B. atropunctata* and *Biscogniauxia sinensis*. To further compare the morphological characteristics of these two species [49], we found that the conidia size of isolates SC1 to SC5 are different to those of *B. atropunctata*; they also differed remarkably in their colony morphology and growth rates [49]. The radial growth rate of *B. atropunctata* on OA was 12.8 mm/d, and it was white felty, azonate, had diffuse and ropy margins and became floccose, with greenish-olivaceous or dull green patches. The reverse of *B. atropunctata* was dull green or greenish-olivaceous [49]. Nevertheless, the isolates SC1–SC5 had a growth rate of 9.8 mm/d, which is much slower than that of *B. atropunctata*. The colony of SC3 on OA (Figure 3) was different from that of *B. atropunctata* on morphology and color. The identification results showed that the fungus on *P. thunbergii* differed from *B. atropunctata* and a new species, *Biscogniauxia sinensis*.

Ju et al. (1998) wrote a monograph on the genus *Biscogniauxia*, in which 49 taxa were covered worldwide [50]. In their study, morphological differences among similar genera were discussed, and the critical identifying features among *Biscogniauxia* species were provided. This genus presents a synteny relationship with other related but morphologically different genera, such as *Graphostroma*, *Camillea* and *Obolarina*, in Xylariaceae [39,51,52], while, Wendt et al. (2018) reinstate and amended the family Graphostromataceae [44].

Graphostromataceae comprised *Biscogniauxia*, *Graphostroma*, *Camillea*, *Obolarina*, *Theissenia*, and *Vivantia* [53]. *Biscogniauxia* has been reported from various woody hosts around the world; more than 10 new hosts have been found in relevant studies recorded in the fungi database of the USDA [54]. *Biscogniauxia* was found in *Malus*, *Mangifera*, *Prunus*, *Pyrus*, and *Vitis* fruit trees. Most of these hosts are angiosperms, but *B. atropunctata* has been isolated from *Juniperus virginiana* in the United States [55]. Meanwhile, *B. mediterranea* usually occurs on *Quercus suber* in the Mediterranean basin [56,57]. But *B. mediterranea* has been reported as a pathogen of *Pinus sylvestris* in Spain [58]. In 2020, it was also isolated from a twig of *Abies alba* with needle browning symptoms in Poland [59]. This fungus has long been considered as an endophyte in all aerial organs (rarely in leaves) of oak trees and has an incubation period without symptoms [60]. However, when the host is weakened or stressed by other pathogens, *B. mediterranea* can become a facultative pathogen; it can accelerate the decline of the tree and eventually lead to the death of the hosts [61–63]. Similar study also indicates that, as an endophyte, it lies dormant within Scots pine (*Pinus sylvestris*) and can influence host growth, leading to slower growth rates in the pine trees [64]. *Biscogniauxia nummularia* is recognized as an endophyte in dicotyledonous angiosperms and some grass species [49]. In 2019, *B. nummularia* was first recorded in southern Poland as an endophyte of white fir (*Abies alba*) and *Pinus* × *rhaetica* Brugger [65,66]. Research has illuminated the endophytic characteristics of *B. nummularia*, enabling it to swiftly transition from a benign endophyte to a primary pathogen [67–69]. Similarly, *Biscogniauxia*, typically found in woody plants, has also been isolated from pines such as *Pinus koraiensis*, firs such as *Abies nephrolepis*, and Douglas fir, as well as from *Taxus cuspidata* as an endophyte [70].

Endophytes usually reside within the internal tissues of plants without causing apparent harm to the host [71]. Due to imbalances in nutrient exchange, environmental changes, and change in host, endophytes can transit into pathogens under such circumstances [72]. *Biscogniauxia* is globally distributed, usually acting as an ubiquitous wood decomposer and a common endophyte [69]. There is substantial evidence that *Biscogniauxia* species exist as endophytes within healthy trees and later become pathogenic to plants when adverse stress occurs [70,73]. Although *Biscogniauxia* has been characterized as an endophytic fungus, evidence from several studies indicate that these endophytes, akin to pathogenic bacteria, possess intrinsic virulence factors and exhibit prolonged latent periods. This virulence potential facilitates the establishment of infections in host plants, particularly when they are located in senescent branches or are subjected to environmental stressors [74]. One of the most significant influence factors on the occurrence of *Biscogniauxia* is climate change.

It has been proved that warm temperatures and a prolonged summer drought favor the growth of *Biscogniauxia* species [75]. Most species of *Biscogniauxia* are particularly inclined to affect trees under water stress [76]. *Biscogniauxia sinensis* might act as an endophyte in many plants, potentially existing symbiotically within them. However, it could also function as a plant pathogen, particularly under stressful conditions such as drought. Thus, the application of sanitation and scarification practices along with appropriate fungicides can effectively prevent and reduce the occurrence of the *Biscogniauxia* on oak trees [77]. However, the control of fungi of this genus on Japanese black pine remains to be studied. Next, biocontrol agents and other control measures will be studied for effectively reducing the impact of *Biscogniauxia sinensis* on forests and ecological system.The climatic conditions during summer in Bazhong City, Sichuan Province, are high temperatures and drought, which enhance plant transpiration and trigger stress conditions. These conditions may induce the expression of pathogenic traits of endophytic fungi. Although the isolation of endophytic fungi was not the focus of our study during the initial field survey, it is necessary to conduct further comprehensive research on this phenomenon.

Generally, *Biscogniauxia* is not frequently reported to cause plant diseases in China. In 2008, *B. mandshurica* was found on dead branches of *Malus* sp. in Changbai Mountain, Jilin Province, China [78]. In March 2014, a new species, *B. glaucae*, was found on the dead bark of an unknown plant in Guizhou Province, China [36]. In 2014, *B. petrensis* was found on rock from two karst caves in Guizhou Province, China [79]. In November 2015, *B. dendrobii* was found in *Dendrobium aphyllum* stems from a nursery in Guizhou Province, China [35]. This is the first report that the new species identified here is associated with discolored and withered needles on *P. thunbergii* in forest. The symptoms have affected the potential value of pine trees, influenced the balance of the forest environment, and caused consequential economic and ecological losses [10].

The discovery and classification of the new species *Biscogniauxia sinensis* not only enhances the diversity of the genus but also provides new perspectives on its genetic diversity and evolutionary relationships with other species [80]. It will help us better understand its ecological role and interactions with host plants. Additionally, it aids in research on how these fungi adapt to various environments and hosts, which is crucial for maintaining the health and stability of forest ecosystems.

5. Conclusions

The morphological features, multi-locus phylogeny, and GCPSR analysis were employed to determine *Biscogniauxia sinensis* as a novel species associated with pine needle blight on *P. thunbergii*. The discovery and classification of *Biscogniauxia sinensis* will expand the current knowledge of this genus. It is necessary to conduct further studies on this disease from multiple perspectives (mycology, epidemiology, ecology and evolution, as well as economy). From the practical aspect, future studies should also focus on reducing its potential damage to *P. thunbergii* and forest ecosystems.

Author Contributions: C.Q.: conceptualization, writing—original draft and review and editing, data curation, investigation, methodology and visualization. R.Z.: writing—review and editing, investigation. X.D.: writing—review and editing, project administration, resources and supervision. D.L.: writing—review and editing, supervision. All authors have read and agreed to the published version of the manuscript.

Funding: This project is supported by the National Natural Science Foundation of China 31800543.

Institutional Review Board Statement: Not applicable for studies not involving humans or animals.

Informed Consent Statement: Not applicable.

Data Availability Statement: Data are contained within the article.

Acknowledgments: The authors are very grateful to Mao-Jiao Zhang for her assistance in morphological and phylogenetic analyses.

Conflicts of Interest: The authors declare no conflicts of interest.

References

1. Yang, H.; Wang, Z.; Song, W.; Zhao, Z.; Zhao, Y. Isolation of proanthocyanidins from *Pinus thunbergii* needles and tyrosinase inhibition activity. *Process Biochem.* **2021**, *100*, 245–251. [CrossRef]
2. Tanaka, S.; Tomita, R.; Saijo, H.; Takahashi, K.; Ashitani, T. Growth-inhibitory activity of components in *Cryptomeria japonica* leaves against *Robinia pseudoacacia*. *J. For. Res.* **2020**, *25*, 192–197. [CrossRef]
3. Masaka, K.; Torita, H.; Sato, H.; Kon, H.; Fukuchi, S.M. Decline of *Pinus thunbergii* Parlat. stands due to excess soil moisture caused by a buried andosol layer at a coastal sand site in Hokkaido, northern Japan. *J. For. Res.* **2010**, *15*, 341–346. [CrossRef]
4. Kim, H.; Lee, H.; Lee, J. Studies on the characteristics of growth of *Pinus thunbergii* planted in a Costal Sand Zone. *J. Korean For. Soc.* **2012**, *101*, 656–662.
5. Beccaccioli, M.; Grottoli, A.; Scarnati, L.; Faino, L.; Reverberi, M. Nanopore hybrid assembly of *Biscogniauxia mediterranea* isolated from *Quercus cerris* affected by charcoal disease in an endangered coastal wood. *Microbiol. Resour. Announc.* **2021**, *10*, e0045021. [CrossRef] [PubMed]
6. Xiao, G. Control Measures against Main *Pinus koraiensis* Diseases in Liaoning Province. *Plant Dis. Pests* **2022**, *13*, 5–6. [CrossRef]
7. Hirose, D.; Osono, T. Development and seasonal variations of *Lophodermium* populations on *Pinus thunbergii* needle litter. *Mycoscience* **2006**, *47*, 242–247. [CrossRef]
8. Du, Z. Common diseases of pine needles and comprehensive prevention and control measures. *Mod. Agric. Technol.* **2022**, 31–32.
9. Li, C.D.; Zhu, X.Q.; Han, Z.M. Investigation on brown-spot needle blight of pines in China. *J. Nanjing For. Univ.* **1986**, *29*, 11–18.
10. Ding, X.L.; Zhao, R.W.; Lin, S.X.; Ye, J.R. Morphological and phylogenetic resolution of *Diplodia neojuniperi* emerging *Diplodia* top dieback of *Pinus thunbergii* Parl. in China. *Phyton* **2022**, *91*, 2813–2825. [CrossRef]
11. Huang, L.; Li, Q.C.; Zhang, Y.; Li, D.W.; Ye, J.R. *Colletotrichum gloeosporioides* sensu stricto is a pathogen of leaf anthracnose on evergreen spindle tree (*Euonymus japonicus*). *Plant Dis.* **2015**, *100*, 672–678. [CrossRef] [PubMed]
12. Damm, U.; Mostert, L.; Crous, P.W.; Fourie, P.H. Novel *Phaeoacremonium* species associated with necrotic wood of *Prunus* trees. *Persoonia* **2008**, *20*, 87–102. [CrossRef] [PubMed]
13. Mirabolfathy, M.; Ju, Y.M.; Hsieh, H.M.; Rogers, J.D. *Obolarina persica* sp. nov., associated with dying *Quercus* in Iran. *Mycoscience* **2013**, *54*, 315–320. [CrossRef]
14. White, T.J.; Bruns, T.; Lee, S.J.W.T.; Taylor, J. Amplification and direct sequencing of fungal ribosomal RNA Genes for phylogenetics. In *PCR Protocols: A Guide to Methods and Applications*; Innis, M.A., Gelfand, D.H., Sninsky, J.J., White, T.J., Eds.; Academic Press, Inc.: New York, NY, USA, 1990; pp. 315–322.
15. Carbone, I.; Kohn, L.M. A method for designing primer sets for speciation studies in filamentous ascomycetes. *Mycologia* **1999**, *91*, 553–556. [CrossRef]
16. Lousie, G.N.; Donaldson, G.C. Development of primer sets designed for use with the PCR to amplify conserved genes from Filamentous Ascomycetes. *Appl. Environ. Microbiol.* **1995**, *61*, 1323–1330. [CrossRef] [PubMed]
17. Hsieh, H.M.; Ju, Y.M.; Rogers, J.D. Molecular phylogeny of *Hypoxylon* and closely related genera. *Mycologia* **2005**, *97*, 844–865. [CrossRef] [PubMed]
18. Ju, Y.M.; Rogers, J.D. *A Revision of the Genus Hypoxylon*; APS Press: St. Paul, MN, USA, 1996.
19. Sohrabi, M.; Mohammadi, H.; Armengol, J.; León, M. New report of *Biscogniauxia rosacearum* as a pathogen on almond trees in Iran. *J. Plant Dis. Prot.* **2022**, *129*, 411–417. [CrossRef]
20. Rajpoot, A.; Kumar, V.; Kumari, R.; Singh, T. Molecular Characteristic of Indian Pangolin with Existing Manidae Species Based on Mitochondrial Genes: A Wildlife Forensic Approach. In Proceedings of the 4th International Arab Forensic Sciences & Forensic Medicine Conference, Riyadh, Saudi Arabia, 27–29 November 2018.
21. Hall, T.A. BioEdit: A user-friendly biological sequence alignment editor and analysis program for Windows 95/98/NT. *Nucleic Acids Symp. Ser.* **1999**, *41*, 95–98. [CrossRef]
22. Zhou, Z.C.; Tang, X.Y.; Hu, S.; Zhu, W.Y.; Wu, X.P.; Sang, W.J.; Ding, H.X.; Peng, L.J. First report of gray spot on tobacco caused by *Alternaria alstroemeriae* in China. *Plant Dis.* **2023**, *107*, 2546. [CrossRef]
23. Zhang, D.; Gao, F.; Jakovlić, I.; Zou, H.; Zhang, J.; Li, W.X.; Wang, G.T. PhyloSuite: An integrated and scalable desktop platform for streamlined molecular sequence data management and evolutionary phylogenetics studies. *Mol. Ecol. Resour.* **2020**, *20*, 348–355. [CrossRef]
24. Kalyaanamoorthy; Subha; Minh, B.Q.; Wong; Thomas, K.F.; Haeseler, V.; Arndt; Jermiin; Lars, S. ModelFinder: Fast model selection for accurate phylogenetic estimates. *Nat. Methods* **2017**, *14*, 87. [CrossRef] [PubMed]
25. Zhang, J.-W.; Dong, H.-P.; Hou, L.-J.; Liu, Y.; Ou, Y.-F.; Zheng, Y.-L.; Han, P.; Liang, X.; Yin, G.-Y.; Wu, D.-M.; et al. Newly discovered Asgard archaea Hermodarchaeota potentially degrade alkanes and aromatics via alkyl/benzyl-succinate synthase and benzoyl-CoA pathway. *ISME J.* **2021**, *15*, 1826–1843. [CrossRef]
26. Wan, Y.; Li, D.W.; Si, Y.Z.; Li, M.; Huang, L.; Zhu, L.H. Three new species of *Diaporthe* causing leaf blight on *Acer palmatum* in China. *Plant Dis.* **2023**, *107*, 849–860. [CrossRef] [PubMed]
27. Ronquist, F.; Teslenko, M.; van der Mark, P.; Ayres, D.L.; Darling, A.; Höhna, S.; Larget, B.; Liu, L.; Suchard, M.A.; Huelsenbeck, J.P. MrBayes 3.2: Efficient Bayesian phylogenetic inference and model choice across a large model space. *Syst. Biol.* **2012**, *61*, 539–542. [CrossRef] [PubMed]

28. Rambaut, A. *FigTree v1. 4.0. A Graphical Viewer of Phylogenetic Trees*; Institute of Evolutionary Biology, University of Edinburgh: Edinburgh, UK, 2012.
29. Hsieh, H.M.; Lin, C.R.; Fang, M.J.; Rogers, J.D.; Ju, Y.M. Phylogenetic status of *Xylaria* subgenus *Pseudoxylaria* among taxa of the subfamily Xylarioideae (Xylariaceae) and phylogeny of the taxa involved in the subfamily. *Mol. Phylogenetics Evol.* **2010**, *54*, 957–969. [CrossRef]
30. Crous, P.W.; Akulov, A.; Balashov, S.; Boers, J.; Braun, U.; Castillo, J.; Delgado, M.A.; Denman, S.; Erhard, A.; Gusella, G.; et al. New and Interesting Fungi. *Fungal Syst. Evol.* **2023**, *11*, 109–156. [CrossRef] [PubMed]
31. Sánchez-Ballesteros, J.; González, V.; Salazar, O.; Acero, J.; Portal, M.A.; Julián, M.; Rubio, V.; Bills, G.F.; Polishook, J.D.; Platas, G.; et al. Phylogenetic study of *Hypoxylon* and related genera based on ribosomal ITS sequences. *Mycologia* **2000**, *92*, 964–977. [CrossRef]
32. Pinto, T. The Phyloecology of *Hypoxylon sensu* lato. Master's Thesis, University of California, Berkeley, CA, USA, 2001.
33. Vu, D.; Groenewald, M.; de Vries, M.; Gehrmann, T.; Stielow, B.; Eberhardt, U.; Al-Hatmi, A.; Groenewald, J.Z.; Cardinali, G.; Houbraken, J.; et al. Large-scale generation and analysis of filamentous fungal DNA barcodes boosts coverage for kingdom fungi and reveals thresholds for fungal species and higher taxon delimitation. *Stud. Mycol.* **2019**, *92*, 135–154. [CrossRef]
34. Ju, Y.M.; Rogers, J.D. New and interesting *Biscogniauxia* taxa, with a key to the world species. *Mycol. Res.* **2001**, *105*, 1123–1133. [CrossRef]
35. Ma, X.Y.; Nontachaiyapoom, S.; Hyde, K.D.; Jeewon, R.; Doilom, M.; Chomnunti, P.; Kang, J.C. *Biscogniauxia dendrobii* sp. nov. and *B. petrensis* from *Dendrobium orchids* and the first report of cytotoxicity (towards A549 and K562) of *B. petrensis* (MFLUCC 14-0151) in vitro. *S. Afr. J. Bot.* **2020**, *134*, 382–393. [CrossRef]
36. Li, Q.R.; Gong, X.F.; Zhang, X.; Pi, Y.H.; Long, S.H.; Wu, Y.P.; Shen, X.C.; Kang, Y.Q.; Kang, J.C. Phylogeny of Graphostromataceae with two new species (*Biscogniauxia glaucae* sp. nov. and *Graphostroma guizhouensis* sp. nov.) and new record of *Camillea broomeana* isolated in China. *Arch. Microbiol.* **2021**, *203*, 6119–6129. [CrossRef] [PubMed]
37. Samarakoon, M.C.; Hyde, K.D.; Maharachchikumbura, S.S.N.; Stadler, M.; Gareth Jones, E.B.; Promputtha, I.; Suwannarach, N.; Camporesi, E.; Bulgakov, T.S.; Liu, J.K. Taxonomy, phylogeny, molecular dating and ancestral state reconstruction of Xylariomycetidae (Sordariomycetes). *Fungal Divers.* **2022**, *112*, 1–88. [CrossRef]
38. Maharachchikumbura, S.; Hyde, K.; Jones, E.; McKenzie, E.; Bhat, D.J.; Dayarathne, M.; Huang, S.-K.; Norphanphoun, C.; Senanayake, I.; Perera, R.; et al. Families of Sordariomycetes. *Fungal Divers.* **2016**, *79*, 1–317. [CrossRef]
39. Raimondo, M.L.; Lops, F.; Carlucci, A. Charcoal canker of pear, plum, and quince trees caused by *Biscogniauxia rosacearum* sp. nov. in Southern Italy. *Plant Dis.* **2016**, *100*, 1813–1822. [CrossRef] [PubMed]
40. Travadon, R.; Lawrence, D.P.; Moyer, M.M.; Fujiyoshi, P.T.; Baumgartner, K. Fungal species associated with grapevine trunk diseases in Washington wine grapes and California table grapes, with novelties in the genera *Cadophora*, *Cytospora* and *Sporocadus*. *Frontiers* **2022**, *3*, 1018140. [CrossRef]
41. Okane, I.; Srikitikulchai, P.; Toyama, K.; Læssøe, T.; Sivichai, S.; Hywel-Jones, N.; Nakagiri, A.; Potacharoen, W.; Suzuki, K.-i. Study of endophytic Xylariaceae in Thailand: Diversity and taxonomy inferred from rDNA sequence analyses with saprobes forming fruit bodies in the field. *Mycoscience* **2008**, *49*, 359–372. [CrossRef]
42. Jankowiak, R.; Bilański, P.; Zając, J.; Jobczyk, A.; Taerum, S.J. The culturable leaf mycobiome of *Viscum album* subsp. *austriacum*. *For. Pathol.* **2023**, *53*, e12821. [CrossRef]
43. Vandegrift, R.; Newman, D.S.; Dentinger, B.T.M.; Batallas-Molina, R.; Dueñas, N.; Flores, J.; Goyes, P.; Jenkinson, T.S.; McAlpine, J.; Navas, D.; et al. Richer than Gold: The fungal biodiversity of *Reserva Los* Cedros, a threatened Andean cloud forest. *Bot. Stud.* **2023**, *64*, 17. [CrossRef] [PubMed]
44. Wendt, L.; Sir, E.B.; Kuhnert, E.; Heitkämper, S.; Lambert, C.; Hladki, A.I.; Romero, A.I.; Luangsa-ard, J.J.; Srikitikulchai, P.; Peršoh, D.; et al. Resurrection and emendation of the Hypoxylaceae, recognised from a multigene phylogeny of the *Xylariales*. *Mycol. Prog.* **2018**, *17*, 115–154. [CrossRef]
45. Bashiri, S.; Abdollahzadeh, J.; Evidente, A. Diagnosing and pathogenicity of *Biscogniauxia* species, the causal agents of oak charcoal canker and decline in Zagros forests of Iran. *J. Plant Pathol.* **2022**, *104*, 1011–1025. [CrossRef]
46. Spies, C.F.J.; Mostert, L.; Carlucci, A.; Moyo, P.; van Jaarsveld, W.J.; du Plessis, I.L.; van Dyk, M.; Halleen, F. Dieback and decline pathogens of olive trees in South Africa. *Persoonia* **2020**, *45*, 196–220. [CrossRef]
47. Quaedvlieg, W.; Binder, M.; Groenewald, J.Z.; Summerell, B.A.; Carnegie, A.J.; Burgess, T.I.; Crous, P.W. Introducing the consolidated species concept to resolve species in the Teratosphaeriaceae. *Persoonia* **2014**, *33*, 1–40. [CrossRef]
48. Royse, D.; Baars, J.J.P.; Tan, Q. Current overview of Mushroom production in the world. In *Edible and Medicinal Mushrooms*; Diego, C.Z., Pardo-Giménez, A., Eds.; John Wiley & Sons Ltd.: Hoboken, NJ, USA, 2017; pp. 5–13.
49. Ju, Y.M.; Rogers, J.D.; Martín, F.S.; Granmo, A. The genus *Biscogniauxia*. *Mycotaxon* **1998**, *66*, 1–98.
50. Bahmani, Z.; Abdollahzadeh, J.; Amini, J.; Evidente, A. *Biscogniauxia rosacearum* the charcoal canker agent as a pathogen associated with grapevine trunk diseases in Zagros region of Iran. *Sci. Rep.* **2021**, *11*, 14098. [CrossRef] [PubMed]
51. Pažoutová, S.; Šrůtka, P.; Holuša, J.; Chudíčková, M.; Kolařík, M. The phylogenetic position of *Obolarina dryophila* (Xylariales). *Mycol. Prog.* **2010**, *9*, 501–507. [CrossRef]
52. Peláez, F.; Platas, G.; Sánchez-Ballesteros, J. Molecular phylogenetic studies within the Xylariaceae based on ribosomal DNA sequences. *Fungal Divers.* **2008**, *31*, 111–134.

53. Daranagama, D.A.; Hyde, K.D.; Sir, E.B.; Thambugala, K.M.; Stadler, M. Towards a natural classification and backbone tree for Graphostromataceae, Hypoxylaceae, Lopadostomataceae and Xylariaceae. *Fungal Divers.* **2018**, *88*, 1–165. [CrossRef]
54. Farr, D.F.; Rossman, A.Y. *Systematic Mycology and Microbiology Laboratory-Fungal Databases*; ARS, USDA: Washington, DC, USA, 2023.
55. Hoffman, M.T.; Arnold, A.E. Geographic locality and host identity shape fungal endophyte communities in cupressaceous trees. *Mycol. Res.* **2008**, *112*, 331–344. [CrossRef]
56. Yangui, I.; Boutiti, M.Z.; Vettraino, A.M.; Bruni, N.; Vannini, A.; Jamaâ, M.L.B.; Boussaid, M.; Messaoud, C. *Biscogniauxia mediterranea* associated with cork oak (*Quercus suber*) in Tunisia: Relationships between phenotypic variation, genetic diversity and ecological factors. *Fungal Ecol.* **2019**, *41*, 224–233. [CrossRef]
57. Bußkamp, J.; Bien, S.; Neumann, L.; Blumenstein, K.; Terhonen, E.; Langer, G.J. Endophytic community in juvenile *Acer pseudoplatanus* and pathogenicity of *Cryptostroma corticale* and other associated fungi under controlled conditions. *J. Plant Pathol.* **2024**, *106*, 565–577. [CrossRef]
58. Farr, D.F.; Rossman, A.Y. *United States National Fungus Collections Fungus-Host Dataset*; ARS, USDA: Washington, DC, USA, 2021.
59. Pusz, W.; Baturo-Ciesniewska, A.; Kaczmarek-Pienczewska, A.; Zwijacz-Kozica, T.; Patejuk, K. The mycobiota of needles and shoots of silver fir (*Abies alba* Mill.) with symptoms of *Herpotrichia* needle browning in the Tatra Mts. (Poland). *Ann. For. Res.* **2020**, *63*, 45–56. [CrossRef]
60. Wilson, D.C. Endophyte: The evolution of a term, and clarification of its use and definition. *Oikos* **1995**, *73*, 274–276. [CrossRef]
61. Linaldeddu, B.T.; Sirca, C.; Spano, D.; Franceschini, A. Variation of endophytic cork oak associated fungal communities in relation to plant health and water stress. *For. Pathol.* **2011**, *41*, 193–201. [CrossRef]
62. Marie-Laure, D.L.; Benoit, M.; Louis-Michel, N.; Dominique, P.; Andrea, V. Interactive effects of drought and pathogens in forest trees. *Ann. For. Sci.* **2006**, *63*, 597–612.
63. Vannini, A.; Lucero, G.; Anselmi, N.; Vettraino, A.M. Response of endophytic *Biscogniauxia mediterranea* to variation in leaf water potential of *Quercus cerris*. *For. Pathol.* **2008**, *39*, 8–14. [CrossRef]
64. Sanz-Ros, A.V.; Müller, M.M.; San Martín, R.; Diez, J.J. Fungal endophytic communities on twigs of fast and slow growing Scots pine (*Pinus sylvestris* L.) in northern Spain. *Fungal Biol.* **2015**, *119*, 870–883. [CrossRef]
65. Patejuk, K.; Kaczmarek-Pieńczewska, A.; Baturo-Ciesniewska, A.; Pusz, W. Mycobiota of peat-bog pine (*Pinus* × *rhaetica*) needles in the Stołowe Mountains National Park, Poland. *Nova Hedwig.* **2021**, *112*, 253–265. [CrossRef]
66. Pusz, W.; Baturo-Ciesniewska, A.; Kaczmarek-Pieńczewska, A.; Zwijacz-Kozica, T. The health status of sliver fir (*Abies alba* Mill.) in selected locations of the Tatra national park and the Karkonosze national park. *For. Wood Technol.* **2020**, *19*, 145–152. [CrossRef]
67. Petrini, L.E.; Petrini, O. Xylariaceous fungi as endophytes. *Sydowia* **1985**, *38*, 201–265. [CrossRef]
68. Patejuk, K.; Baturo-Ciesniewska, A.; Pusz, W.; Kaczmarek-Pienczewska, A. *Biscogniauxia* charcoal canker-A new potential threat for Mid-European forests as an effect of climate change. *Forests* **2022**, *13*, 89. [CrossRef]
69. Petrović, E.; Godena, S.; Cosic, J.; Vrandečić, K. Identification and pathogenicity of *Biscogniauxia* and *Sordaria* species isolated from Olive trees. *Horticulturae* **2024**, *10*, 243. [CrossRef]
70. Amand, S.; Langenfeld, A.; Blond, A.; Dupont, J.; Nay, B.; Prado, S. Guaiane sesquiterpenes from *Biscogniauxia nummularia* featuring potent antigerminative activity. *J. Nat. Prod.* **2012**, *75*, 798–801. [CrossRef] [PubMed]
71. Cui, J.M.; Nie, F.X.; Zhao, Y.Q.; Zhang, D.W.; Zhou, D.G.; Wu, J.F.; Qu, L.; Xiao, L.; Liu, L.L. A review on plant endophytes in response to abiotic stress. *Environ. Pollut. Bioavailab.* **2024**, *36*. [CrossRef]
72. Bhunjun, C.S.; Phukhamsakda, C.; Hyde, K.D.; McKenzie, E.H.C.; Saxena, R.K.; Li, Q. Do all fungi have ancestors with endophytic lifestyles? *Fungal Divers.* **2024**, *125*, 73–98. [CrossRef]
73. Nugent, L.K.; Sihanonth, P.; Thienhirun, S.; Whalley, A.J.S. *Biscogniauxia*: A genus of latent invaders. *Mycologist* **2005**, *19*, 40–43.
74. Schulz, B.; Boyle, C. The endophytic continuum. *Mycol. Res.* **2005**, *109 Pt 6*, 661–686. [CrossRef]
75. La Porta, N.; Capretti, P.; Thomsen, I.M.; Kasanen, R.; Hietala, A.M.; Von Weissenberg, K. Forest pathogens with higher damage potential due to climate change in Europe. *Can. J. Plant Pathol.* **2008**, *30*, 177–195. [CrossRef]
76. Granata, G.; Sidoti, A. *Biscogniauxia nummularia*: Pathogenic agent of a beech decline. *For. Pathol.* **2004**, *34*, 363–367. [CrossRef]
77. Karami, J.; Kavosi, M.R.; Babanezhad, M.; Kiapasha, K. Integrated management of the charcoal disease by silviculture, chemical and biological methods in forest parks. *J. Sustain. For.* **2017**, *37*, 429–444. [CrossRef]
78. Vasilyeva, L.; Li, Y.; Stephenson, S. Some pyrenomycetous fungi new to China. *Mycotaxon* **2009**, *109*, 415–428. [CrossRef]
79. Zhang, Z.F.; Liu, F.; Zhou, X.; Liu, X.Z.; Liu, S.J.; Cai, L. Culturable mycobiota from Karst caves in China, with descriptions of 20 new species. *Persoonia* **2017**, *39*, 1–31. [CrossRef] [PubMed]
80. Chen, M.L.; Zhang, J.Y.; Xiao, Y.P.; Lu, Y.Z. *Biscogniauxia dicranopteridis* sp. nov. and *B. petrensis* isolated from *Dicranopteris dichotoma* in China. *Phytotaxa* **2024**, *641*, 255–266. [CrossRef]